This is a postprint of an article published in
Rinas, U., Hoffmann, F., Betiku, E., Estape, D., Marten, S.
Inclusion body anatomy and functioning of chaperone-mediated in vivo inclusion body disassembly during high-level recombinant protein production in Escherichia coli
(2007) Journal of Biotechnology, 127 (2), pp. 244-257.

Inclusion body anatomy and functioning of chaperone-mediated *in-vivo* inclusion body disassembly during high-level recombinant protein production in *Escherichia coli*

Ursula Rinas[a,*], Frank Hoffmann[b], Eriola Betiku[a], David Estapé[a], and Sabine Marten[a]

[a] Biochemical Engineering Division, GBF German Research Center for Biotechnology, Mascheroder Weg 1, D-38124 Braunschweig, Germany

[b] Institut für Biotechnologie, Martin-Luther-Universität Halle-Wittenberg, Kurt-Mothes-Str. 3, D-06120 Halle, Germany

[*] Corresponding author: Tel: 0049-531-6181-126; Fax: 0049-531-6181-111,

e-mail: URI@gbf.de

Running title: inclusion body disaggregation

Keywords: inclusion bodies, disaggregation, chaperones, recombinant protein production

Abstract. During production in recombinant *E. coli*, the human basic fibroblast growth factor (hFGF-2) partly aggregates into stable cytoplasmic inclusion bodies. These inclusion bodies additionally contain significant amounts of the heat-shock chaperone DnaK, and putative DnaK substrates such as the elongation factor Tu (ET-Tu) and the metabolic enzymes dihydrolipoamide dehydrogenase (LpdA), tryptophanase (TnaA), and D-tagatose-1,6-bisphosphate aldolase (GatY). Guanidinium hydrochloride induced disaggregation studies carried out *in vitro* on artificial aggregates generated through thermal aggregation of purified hFGF-2 revealed identical disaggregation profiles as hFGF-2 inclusion bodies indicating that the heterogenic composition of inclusion bodies did not influence the strength of interactions of hFGF-2 in aggregates formed *in vivo* as inclusion bodies compared to those generated *in vitro* from native and pure hFGF-2 through thermal aggregation. Compared to unfolding of native hFGF-2, higher concentrations of denaturant were required to dissolve hFGF-2 aggregates showing that more energy is required for disruption of interactions in both types of protein aggregates compared to the unfolding of the native protein. *In vivo* dissolution of hFGF-2 inclusion bodies was studied through coexpression of chaperones of the DnaK and GroEL family and ClpB and combinations thereof. None of the chaperone combinations was able to completely prevent the initial formation of inclusion bodies, but upon prolonged incubation mediated disaggregation of otherwise stable inclusion bodies. The GroEL system was particularly efficient in inclusion body dissolution but did not lead to a corresponding increase in soluble hFGF-2 rather was promoting the proteolysis of the recombinant growth factor. Coproduction of the disaggregating DnaK system and ClpB in conjunction with small amounts of the chaperonins GroELS was most efficient in disaggregation with concomitant formation of soluble hFGF-2. Thus, fine-balanced coproduction of chaperone combinations can play an important role in the production of soluble recombinant proteins with a high aggregation propensity not through prevention of aggregation but predominantly through their disaggregating properties.

1. Introduction

Inclusion bodies are protein aggregates that often form during overproduction of recombinant proteins. They have long been regarded as a localized mass of unordered polypeptide chains but more recent research suggested that these proteins may also have defined conformations within the aggregated state (Ventura and Villaverde, 2006). Inclusion bodies also have long been considered inert towards *in vivo* dissolution, but it is now generally accepted that inclusion body proteins can be solubilized *in vivo* concomitant to or followed by proteolytic degradation (Corchero et al., 1997, Carrió et al., 1999; Cubarsí et al., 2001; LeThanh et al., 2005; Vera et al., 2005) or even by folding into the native state (Carrió and Villaverde, 2001; LeThanh et al., 2005).

Comparable observations have been made with endogenous proteins aggregated by heat-shock in *E. coli* which resolubilize when cells are subjected to lower temperature (Kędzierska et al., 1999). Similarily to solubilized inclusion body proteins, the resolubilized proteins from endogenous heat-shock aggregates can reach their native conformation (Kędzierska et al., 2001) or are subjected to proteolytic degradation (Laskowska et al., 1996). The dissolution of these endogenous aggregates depends on the presence of chaperones, in particular on chaperones of the DnaK family (Kędzierska et al., 1999).

Chaperones involved in the coordinated dissolution of protein aggregates form an interlinked network, which includes the Hsp70-chaperone DnaK and the AAA+ protein ClpB (Mogk et al., 2003a; Weibezahn et al., 2004; 2005). Both DnaK and ClpB are essential for removal of heat-shock aggregates, but high levels of DnaK can compensate a lack of ClpB due to partially overlapping functions (Kędzierska et al., 1999; Kędzierska and Matuszewska, 2001; Laskowska et al., 1996; Thomas and Baneyx, 2000). *In vitro* experiments revealed that DnaK can solubilize small aggregates alone but requires cooperation with ClpB for solubilization of larger aggregates (Diamant et al., 2000; Goloubinoff et al., 1999; Zolkiewski, 1999). The

chaperonins GroEL and GroES are also involved in removal of heat-shock aggregates at lower temperature (Kędzierska et al., 1999); a direct role of GroELS in disaggregation, however, has been excluded (Mogk et al., 1999). Rather, it has been suggested that GroELS is involved in promoting folding and refolding of newly synthesized and misfolded proteins (Mogk et al., 1999) and, if folding and refolding is not possible, is involved in promoting the degradation of unstable and abnormal proteins (Kandror et al., 1994, 1999).

Coproduction of chaperones of the DnaK and GroEL family with recombinant proteins has been traditionally examined with the goal to increase the amount of soluble protein (e.g. Goloubinoff et al., 1989; Blum et al., 1992; Georgiou and Valax, 1996; Nishihara et al., 1998; Baneyx and Palumbo, 2002). Although the substrate specificity of these chaperone systems has been characterized and an enormous progress in understanding chaperone mediated protein folding processes has been achieved, the success of chaperone coproduction on increasing soluble protein accumulation is still a trial-and-error process and cannot be predicted from properties of the recombinant protein (Hoffmann and Rinas, 2004; Baneyx and Mujacic, 2004; Ventura and Villaverde, 2006). Moreover, in some cases, e.g. during overexpression of *dnaK*, even stabilization of inclusion bodies can occur, most presumably by downregulation of the heat-shock response including a reduced synthesis of other heat-shock chaperones and proteases (Petersson et al., 2004). Chaperones of the DnaK and GroEL family also associate with inclusion bodies. DnaK is localized preferentially on the surface of inclusion bodies (Carrió and Villaverde, 2005) and, together with ClpB, is recovered with smaller protein aggregates during sucrose density centrifugation (Schrödel and de Marco, 2005). GroEL, on the other hand, is homogeneously distributed in the cytosol, absent from the inclusion body surface, but found in minor amounts also inside of inclusion bodies (Carrió and Villaverde, 2005). During *in vitro* recovery by sucrose density centrifugation, GroEL is recovered with larger protein aggregates (Schrödel and de Marco, 2005). The exact function of the chaperones of the DnaK and GroEL family in inclusion body metabolism is not yet

understood; e.g. experimental results are even compatible with an active role of GroEL in the deposition of misfolded protein into inclusion bodies (Carrió and Villaverde, 2003). Production of the human basic fibroblast growth factor (hFGF-2) using a temperature-inducible expression system results in the formation of soluble growth factor as well as in the formation of inclusion bodies (Seeger et al., 1995). hFGF-2 is a protein of 155 amino acids, sufficiently small to be incorporated into the central cavity formed by the two stacked homoheptameric GroEL rings (Sakikawa et al., 1999; Houry et al., 1999). It is a protein of low stability, in particular under non-reducing conditions (Estapé et al., 1998) and exhibits very slow folding kinetics (Estapé and Rinas, 1999). Temperature-induced production of hFGF-2 initially leads to the accumulation of hFGF-2 exclusively in the aggregated form (Hoffmann and Rinas, 2000). Accumulation of soluble hFGF-2 starts with a delay after heat-shock protein synthesis reached their peak level (Hoffmann and Rinas, 2000). Modelling data indicate that the soluble state might be reached only after *in vivo* refolding from the aggregated state (Hoffmann et al., 2001).

In this study we aimed for a detailed analysis of the anatomy of inclusion bodies produced during temperature-induced synthesis of hFGF-2 by identifying integral inclusion body contaminants and by investigating the cohesive forces amongst inclusion body proteins through a comparative study on the resistance of inclusion body proteins, *in vitro* generated protein aggregates and native protein towards chemical denaturants. Moreover, we also aimed for a mechanistic understanding of the function of individual molecular chaperones in the inclusion body assembly/disassembly process by producing the recombinant protein in chaperone mutant strains as well as in strains coproducing chaperones of the DnaK and GroEL family and the AAA+ chaperone ClpB and combinations thereof.

2. Material and Methods

2.1. Host strains, plasmids, and culture conditions

Escherichia coli strains used in this study are TG1 (DSM 6056) and MC4100 *araD139 Δ(argF-lac) U169 rpsL150 relA1 flbB5301 deoC1 ptsF25 rbsR* and its chaperone mutants as listed in Table 1. The human basic fibroblast growth factor (hFGF-2) is encoded on the plasmid pλFGFB, which is derived from the expression vector pCYTEXP1 (Seeger et al., 1995). Gene expression from the strong promoter tandem $\lambda P_R P_L$ is controlled by the thermolabile repressor cI857 also encoded on the plasmid. Both plasmids also carry the *amp* gene coding for resistance against ampicillin. Plasmids for coproduction of chaperones are listed in Table 2.

High-cell density cultures were carried out as described previously (Seeger et al., 1995). To test the effect of chaperone coexpression or absence, cells were grown in shake flask cultures (50 ml medium in 250 ml Erlenmeyer flasks) using a defined glucose-mineral salt medium (Korz et al., 1995) supplemented with the appropriate antibiotics at 30°C to an OD_{600} of 0.5. The synthesis of hFGF-2 was induced by temperature-shift to 42°C. Induction of chaperones was independent of hFGF-2 synthesis, they were induced by addition of 0.5 mmol L^{-1} isopropyl-β-D-galactopyranoside (IPTG) either one hour before or one hour after induction of hFGF-2. All experiments were carried out at least in duplicate.

2.2. Protein fractionation and one-dimensional SDS-PAGE analysis

Culture samples were centrifuged (Biofuge A, Heraeus Instruments Holding, Hanau) at 13,000 rpm for 5 min, after removal of the supernatant cell pellets were stored at –70°C until further analysis. Before disruption of cells, the cell pellet was resuspended in 50 mmol L^{-1} sodium phosphate buffer (pH 7) to an OD_{600} of 5. Afterwards, cells were disrupted by sonication (50kHz, LabSonic 2000U, B. Braun International, Melsungen) for 3 min and this was taken as total cell protein. 200 µL of the total cell protein were centrifuged (Biofuge 28 RS, Heraeus Instruments Holding, Hanau) at 4°C, 22,000 rpm for 30 min, the supernatant

served as soluble cell protein. The pellet was resuspended in an equal volume of the phosphate buffer and centrifugation repeated. Insoluble cell protein was collected by resuspension of the pellet in 50 µL of phosphate buffer (i.e. concentrated four times). All preparations were carried out on ice to prevent protein degradation and aggregation. One-dimensional SDS-PAGE analysis was carried out using precast gels (Tris-HCl 8-16%, Bio-Rad Criterion™ System, Bio-Rad Laboratories GmbH, München, Germany) according to the manufacturers instructions. Gels were stained with Coomassie Brilliant Blue R250, and quantification was carried out by densitometry (Quantiscan, Biosoft Cambridge, UK).

2.3. Two-dimensional gel electrophoresis and protein identification

Two-dimensional equilibrium (Rinas and Bailey, 1992) and non-equilibrium electrophoresis (Hoffmann and Rinas, 2000) were carried out as described previously. Spot identification was either done by N-terminal sequence analysis and/or by Maldi-ToF (GKIIGIDLGT: DnaK; AAKDVKFGND: GroEL; STKKKPLTQEQLEDARRLKA: repressor cI857; M?LPV?EF?DA?: SdhA; MYVVSTKQMLNNAQRGGY?V: GatY; STEIKTQVVV: LpdA; MENFKHLPEPFRIRVIEPVK: TnaA; EF-Tu: acetylated N-terminus, identification only by Maldi-ToF).

2.4. Guanidine-hydrochloride induced unfolding and disaggregation studies.

hFGF-2 was purified from the soluble cell fraction as described previously (Seeger and Rinas, 1996). Guanidine-hydrochloride (Gdn-HCl) induced unfolding studies of native hFGF-2 based on changes in fluorescent properties were performed as described (Estapé et al., 1998). Thermal unfolding of hFGF-2 was studied by a gradual temperature increase [0.1 to 0.3°C per minute, 10 µg mL^{-1} hFGF-2 in 100 mmol L^{-1} sodium phosphate buffer (pH 7) in the presence or absence of 100 mmol L^{-1} β-mercaptoethanol]. Unfolding was monitored by measurement of the protein fluorescence emission at 355 nm (excitation at 280 nm) as described previously (Estapé et al., 1998).

For disaggregation studies of pure hFGF-2 aggregates, pure hFGF-2 (5 mL of 0.2 mg mL^{-1} hFGF-2 in sodium phosphate buffer) was subjected to 70°C for one hour to promote aggregation. The resulting suspension was centrifuged at 25,000 *g* for two hours at 4°C. The supernatant was discarded and the pellet was resuspended by sonication on ice in 8 mL sodium phosphate buffer. Aliquots (100 μL) of this suspension were mixed with varying concentrations of Gdn-HCl (± 100 mmol L^{-1} β-mercaptoethanol in sodium phosphate buffer, 1 mL final volume). Soluble and insoluble fractions were obtained after subsequent centrifugation at 15,000 *g* for one hour. The amount of solubilized hFGF-2 was determined by fluorescence emission at 355 nm (excitation 280 nm) as described previously (Estapé et al., 1998).

Crude inclusion bodies obtained from high-cell-density cultures (Seeger et al., 1995; Estapé and Rinas, 1996) were resuspended by sonication on ice in the presence of varying concentrations of Gdn-HCl in sodium phosphate buffer (1 mg mL^{-1} final hFGF-2 concentration). Soluble and insoluble fractions were obtained after subsequent centrifugation at 15,000 *g* for 1 hour, analyzed by SDS-PAGE and quantified by densitometry.

3. Results

3.1. Inclusion body anatomy

3.1.1. Protein compositional analysis of hFGF-2 inclusion bodies

hFGF-2 was produced in high-cell density fed-batch cultures using a temperature-inducible expression system (Seeger et al., 1995). The insoluble cell proteome containing hFGF-2 inclusion bodies was analyzed by two-dimensional gel electrophoresis (Fig. 1A and C) and compared to the insoluble proteome of the control strain carrying the "empty" expression vector grown under identical conditions (Fig. 1B and D).

Common to the insoluble proteome of both strains are the plasmid encoded repressor cI857 (Fig. 1C and D), which aggregated presumably because of its thermolability, and membrane proteins such as the flavoprotein subunit of succinate dehydrogenase, SdhA (Fig. 1C and D) present in the inner cell membrane, and the outer membrane proteins OmpA, OmpF, and OmpC (Fig. 1A and B). All these proteins are detected in comparable amounts in the producing (Fig. 1A and C) as well as in the control strain (Fig. 1B and D). The outer membrane proteins are components of the cell debris which can be removed from inclusion bodies by detergent washing (data not shown).

Proteins not detected in the insoluble cell fraction of both strains (Fig. 1A, positions indicated by gray arrows), although they have been identified as integral components of inclusion bodies in other cases, are pre-β-lactamase, the precursor of the enzyme conferring resistence to ampicillin in plasmid-carrying strains (Hart et al., 1990; Kane and Hartley, 1991; Rinas and Bailey, 1993), the small heat-shock proteins IbpA and IbpB (Allen et al., 1992) and GroEL (Schrödel et al., 2005). Synthesis of pre-β-lactamase (Hoffmann and Rinas, 2001a) and the small heat shock proteins IbpA and IbpB (Hoffmann and Rinas, 2000) is too low to cause coaggregation into hFGF-2 inclusion bodies. Concerning the absence of GroEL in hFGF-2

inclusion bodies, we speculate that the small size of hFGF-2 allows its complete entry into the central pore of GroEL thereby preventing protrusion of unprotected and unfolded parts which else might became entangled into inclusion bodies together with the attached chaperone (for details refer to Discussion).

Proteins that specifically aggregate during production of hFGF-2 include the elongation factor Tu (EF-Tu), a house keeping protein also detected in other inclusion bodies (Hart et al., 1990). Moreover, metabolic proteins such as dihydrolipoamide dehydrogenase (LpdA), which is a component of the pyruvate and 2-oxoglutarate dehydrogenase complex and tryptophanase (TnaA), specifically aggregate in hFGF-2 producing cells (Fig. 1C) but not in the respective control strain grown under identical conditions (Fig. 1D). The synthesis of both proteins is upregulated under these culture conditions (Hoffmann et al., 2002), their presence in inclusion bodies, however, has to our knowledge not been reported before. Another protein found exclusively in the insoluble cell fraction of hFGF-2 producing cells was identified as D-tagatose-1,6-bisphosphate aldolase (GatY) (Fig. 1C). This protein has been also identified in the inclusion bodies of other recombinant proteins (Josef Lengeler and Peter Neubauer, personal communication). Moreover, the chaperone DnaK was detected in significantly higher amounts in the insoluble proteome of hFGF-2 producing cells (Fig. 1A and C).

3.1.2. Resistance of inclusion body proteins, in vitro *generated aggregates and native hFGF-2 towards denaturants*

To evaluate the propensity of hFGF-2 to from inclusion bodies the soluble as well as aggregated variants of the protein were subjected to stability analysis.

Native hFGF-2 purified to homogeneity from the soluble cell fraction (Seeger and Rinas, 1996) was subjected to increasing concentrations of the chaotropic agent guanidinium hydrochloride (Gdn-HCl) for unfolding studies under reducing conditions (Estapé et al., 1998; Fig. 2A). Unfolding of native hFGF-2 took place at a midpoint of 1.1 mol L^{-1} Gdn-HCl

corresponding to a low free energy of unfolding, $\Delta G_{app}^{H_2O} \approx 20$ kJ mol^{-1} (Estapé et al., 1998). In comparison, aggregates of hFGF-2 generated *in vitro* by subjecting native hFGF-2 to 70°C or recovered as *in vivo* produced inclusion bodies using the temperature-inducible expression system were also subjected to increasing concentrations of Gdn-HCl under reducing conditions (Fig. 2A). The dissolution profiles for both types of hFGF-2 aggregates were very similar. Thus, the heterogenic composition of inclusion bodies (Fig. 1) did not influence the strength of interactions of hFGF-2 in aggregates formed *in vivo* as inclusion bodies compared to those generated *in vitro* from native and pure hFGF-2 through thermal aggregation. The midpoint of dissolution for both types of aggregates was located at 2.7 mol L^{-1} Gdn-HCl (Fig. 2A), clearly showing that the concentrations of chaotropic agent needed for disruption of interactions in both types of protein aggregates were much higher than the concentration required for the unfolding of the native protein.

In addition to chemical unfolding of hFGF-2, temperature-induced unfolding of native hFGF-2 was studied under reducing and also under non-reducing conditions (Fig. 2B). Under reducing conditions, a sharp transition from the folded to the unfolded state was found above 50°C, whereas a broad unfolding transition range started already above 30°C in the absence of a reducing agent (Fig. 2B). Thermal denaturation was irreversible and resulted in formation of aggregates that could not be dissolved upon sole temperature reduction (not shown).

3.2. Role of chaperones during assembly and disassembly of inclusion bodies

3.2.1. Impact of DnaKJ/GrpE or GroELS coproduction on hFGF-2 inclusion body metabolism

During production at 42°C, hFGF-2 reached a concentration of 75 mg per gram cell dry mass within one hour with one third accumulating in the insoluble cell fraction; neither amount nor distribution pattern changed subsequently during the observation period of eight hours (Fig.

3A). Thus, the net amount of hFGF-2 within the inclusion bodies remained unchanged in the absence of chaperone coproduction.

To study the impact of chaperones on the prevention or dissolution of inclusion bodies, coproduction of DnaKJ/GrpE or GroELS was examined. Chaperone genes were placed on compatible plasmids and induction of chaperone synthesis was independent of hFGF-2 synthesis.

Expression of chaperone genes (DnaKJ/GrpE or GroELS) was chemically induced one hour before or one hour after the induction of hFGF-2 by temperature upshift.

Neither the DnaKJ/GrpE nor the GroELS system was able to prevent the formation of hFGF-2 inclusion bodies (Figs. 3 and 4, respectively). But both chaperone systems were able to dissolve inclusion bodies. While coexpression of the DnaKJ/GrpE system was only leading to partial disaggregation of hFGF-2 inclusion bodies (Fig. 3), coexpression of GroELS was leading to almost complete inclusion body dissolution (Fig. 4). However, dissolution of inclusion bodies during coexpression of the GroELS system did not lead to a corresponding increase of soluble hFGF-2 (Fig. 4). Thus, in this system dissolution of hFGF-2 inclusion bodies through GroELS was resulting in the proteolysis of the recombinant growth factor. During coexpression of the DnaKJ/GrpE system, the amount of soluble hFGF-2 was neither positively nor negatively affected (Fig. 3).

3.2.2. Impact of combined chaperone coproduction on initial accumulation of hFGF-2 in soluble and inclusion body fractions

As coproduction of DnaKJ/GrpE or GroELS alone did not improve the amount of soluble hFGF-2, combinations of different chaperone systems were investigated. In addition to combined coproduction of DnaKJ/GrpE and GroELS, coproduction of the disaggregation chaperone ClpB was also examined.

The synthesis of DnaKJ/GrpE, GroELS (in large amounts: LS, in small amounts: ls), ClpB or combinations thereof was chemically induced one hour before the induction of hFGF-2 by temperature upshift. Overproduction of DnaKJ/GrpE + ClpB or DnaKJ/GrpE + ClpB + GroELS (ls) reduced the initial accumulation of insoluble hFGF-2, i.e. the concentration one hour after the temperature shift, by 60%, whereas DnaKJ/GrpE without ClpB had nearly no effect on hFGF-2 accumulation, neither in the soluble nor in the inclusion body fraction (Fig. 5). Again, none of the chaperone combinations was able to completely prevent the formation of inclusion bodies. The highest amount of soluble hFGF-2 was reached in the system where DnaKJ/GrpE and ClpB were coexpressed, however, the amount of soluble hFGF-2 produced within the first hour with coexpression of these chaperones did not surpass the amount of soluble hFGF-2 in the absence of chaperone coexpression.

3.2.3. Impact of combined chaperone coproduction on longterm accumulation of hFGF-2 in soluble and inclusion body fractions

The longterm effect of combined chaperone coexpression was examined between 4-8 h after induction of hFGF-2 synthesis when the culture had reached stationary levels of product and chaperones.

All chaperone systems mediated the dissolution of already formed hFGF-2 inclusion bodies during further incubation at 42°C, even when they were induced one hour after induction of hFGF-2 synthesis (Fig. 6A). Again, the GroELS-based systems were most efficient leading to almost complete dissolution of hFGF-2 inclusion bodies (Fig. 6A). A large excess of GroELS was required for removal of aggregates, as the inclusion bodies were more stable when GroELS was coproduced in smaller amounts (Fig. 6A). Coexpression of DnaKJ/GrpE or DnaKJ/GrpE + ClpB was less efficient, reducing the amount of hFGF-2 in the insoluble cell fraction by only 40% compared to the reference cultivation without coproduction of chaperones (Fig. 6A).

A significant increase in the amount of soluble hFGF-2 during longterm incubation was only observed in the culture coexpressing all chaperones [DnaKJ/GrpE + ClpB and GroELS (ls)]. In this case the amount of soluble hFGF-2 increased by 40% compared to the culture without chaperone coexpression (Fig 6B). However, this increase was only observed when chaperone induction occurred before induction of hFGF-2 synthesis. Coexpression of DnaKJ/GrpE + ClpB (without GroELS) had a slight positive effect on the amount of soluble growth factor during longterm incubation (Fig. 6B). But again, this was only observed when chaperone induction occurred before induction of hFGF-2 synthesis. Coexpression of DnaKJ/GrpE alone had no significant effect on the amount of soluble growth factor during longterm incubation (Fig. 6B). Systems based on the coexpression of large amount of GroELS [DnaKJ/GrpE + ClpB +GroELS (LS) or GroELS (LS) alone] even decreased the concentration of soluble hFGF-2 by 20 or 40%, respectively (Fig. 6B) corroborating again the degradation promoting effect of the GroELS system.

3.2.4. Production of hFGF-2 in chaperone mutant strains

The above results revealed a critical role of the disaggregating chaperones DnaKJ/GrpE and ClpB in the generation of soluble hFGF-2 while the chaperonins GroELS where not promoting the formation of soluble hFGF-2 but instead were promoting its degradation. We thus investigated production of hFGF-2 and its partitioning into soluble and insoluble cell fractions in strains carrying deletions or conditional mutations of these chaperones genes. Production of hFGF-2 in strains with a deletion of *groES* or conditional mutations in *groEL* did not change the distribution of hFGF-in soluble and insoluble cell fractions although the total amount of recombinant protein decreased in the mutant strains (Fig. 7). This clearly shows that the GroELS chaperonins are not essential for the formation of soluble hFGF-2. In contrast, deletion mutants of *dnaK* or *clpB*, or in particular the double deletion mutant,

revealed a drastic reduction in the amount of soluble growth factor clearly demonstrating the vital role of these chaperones for the generation of soluble hFGF-2 (Fig. 7).

4. Discussion

Traditionally, protein aggregation has been attributed to unidirectional kinetic competition of folding and aggregation reactions (Kiefhaber et al., 1991). More recent work, however, indicated that *in vivo* a dynamic equilibrium between soluble and insoluble states exists (Carrió and Villaverde, 2001).

Aggregates of hFGF-2 generated *in vitro* or *in vivo* are more stable than the native growth factor towards chemical denaturants. Moreover, *in vitro* studies show that hFGF-2 is easily denatured both by chaotropic agents (Estapé et al., 1998) and by heat, in particular under non-reducing conditions where denaturation already starts at the temperature used for the production of this growth factor. Thus, a potential equilibrium between soluble and insoluble states is biased towards the aggregated state.

Removal of aggregated protein was enhanced most efficiently by overproduction of GroELS: hFGF-2 that has accumulated as inclusion bodies was almost completely removed three hours after induction of GroELS overproduction (Fig. 4). As hFGF-2 is also removed from the soluble cell fraction, GroELS seems to promote degradation. As the GroELS system is not directly involved in protein disaggregation we can interpret the role of GroELS as a mediator between aggregated and soluble states. hFGF-2 is sufficiently small to be incorporated into the central cavity of the GroEL multimer, and thus can be effectively protected from intermolecular interaction with other misfolded hFGF-2 molecules, a subsequent release into unfavourable conditions will then lead to degradation. On the first sight seemingly contradicting results with large fusion proteins where an active role of GroEL in inclusion body buildup has been proposed (Carrió and Villaverde, 2003) are in line as in that case the recombinant protein is too large to be incorporated into the GroEL cavity and thus protruding parts of the recombinant protein can cause intermolecular interactions leading to intracellular aggregation and inclusion body buildup. Moreover, the presence of GroEL has been shown in

the inclusion bodies of large proteins (Carrió and Villaverde, 2005; Schrödel and de Marco, 2005). In contrast, in hFGF-2 containing inclusion bodies GroEL is absent corroborating the above conclusion.

For generation of soluble hFGF-2, the DnaK system and ClpB were found to be essential. While deletion or mutation of the other chaperone genes show minor impact on the partitioning of hFGF-2 into soluble and insoluble cell fractions, with two thirds of hFGF-2 accumulating in the soluble fraction as in wildtype cells, only a minor part of hFGF-2 was soluble in the *clpB* and *dnaK* deletion strains, pointing out the requirement for these particular chaperones. However, DnaKJ/GrpE overproduction was not sufficient to prevent hFGF-2 aggregation under the conditions employed in this study, even when induced one or four hours (not shown) before induction of hFGF-2. One the other hand, inclusion bodies formed prior or concomitant to overproduction of DnaK are dissolved at least partly afterwards, whereas the inclusion bodies were stable for at least eight hours without chaperone overproduction. Thus, reversion and not prevention of aggregation is the main role of the DnaK system during production of hFGF-2. The efficacy of the DnaK system in disaggregating inclusion body proteins might be additionally influenceable by the ratio of DnaK, DnaJ, and GrpE, as in our case the individual components of the DnaK family were synthesized in a non-stoichiometric ratio with an excess of DnaK (cf. Fig.3). On the other hand, overproduction of ClpB in addition to DnaKJ/GrpE significantly reduced accumulation of hFGF-2 in the insoluble cell fraction, directly after induction of hFGF-2 synthesis and during longterm production indicating that ClpB does not only disaggregate but also prevents the formation of aggregates. In contrast to the coexpression of the GroELS system, overproduction of ClpB in addition to DnaKJ/GrpE also enhanced the accumulation of soluble hFGF-2, especially in conjunction with overproduction of GroELS in small amounts. This finding supports the hypothesis by Thomas and Baneyx (2000) that ClpB can also facilitate *de novo* folding. However, we can not completely exclude that the reduced growth

rate in response to induction of chaperone gene expression (data not shown) also caused reduced hFGF-2 synthesis rates thereby favourably affecting the formation of soluble growth factor. On the other hand, growth rate reduction were similar in strains coproducing DnaKJ/GrpE alone or in combination with ClpB and small amounts of GroELS, thus, supporting the conclusion that ClpB is at least partly involved in facilitating *de novo* protein folding at the conditions investigated.

Thus, the disaggregating DnaK system and ClpB were identified as the limiting factors for the production of soluble hFGF-2. This is also corroborated by the finding that the disaggregating chaperone DnaK was detected at elevated levels in hFGF-2 inclusion bodies. The majority of proteins that are located in the insoluble cell fraction specifically of hFGF-2 producing cells are in the rage of 30 to 75 kDa (Fig. 1A and C), a size preferentially bound by DnaK (Teter et al., 1999). In particular, several components of the hFGF-2 inclusion bodies have been identified as DnaK substrates, e.g. the thermolabile protein GatY (Mogk et al., 1999), EF-Tu (Malki et al, 2002; Vorderwülbecke et al., 2004) and TnaA as well as LpdA (Vorderwülbecke et al., 2004). Thus, most of the specifically aggregating proteins are DnaK substrates, corroborating the lack of this chaperone during hFGF-2 production. Moreover, this study also shows that disaggregation can play an important role in the production of soluble recombinant proteins, as previously proposed by a quantitative model of inclusion body formation (Hoffman et al., 2001).

Acknowledgements

Eriola Betiku gratefully acknowledges financial support by the Deutscher Akademischer Austauschdienst (DAAD). We are also grateful to Bernd Bukau, Axel Mogk. and Francois Baneyx for the kind donation of plasmids and strains. Moreover, we thank Rita Getzlaff for N-terminal protein sequencing and Manfred Nimtz for Maldi-ToF analysis of tryptic digests.

Tables

Table 1: Plasmids encoding the molecular chaperones investigated in this study.

Plasmid	Description†	Reference
pBB528	pSC101 *ori*, encoding *lacI*^{q} (cm^{r})	Tomoyasu et al. (2001)
pBB530	pSC101 *ori*, encoding *grpE* (spec^{r})	Tomoyasu et al. (2001)
pBB535	p15A *ori*, encoding *dnaK*, *dnaJ* (spec^{r})	Tomoyasu et al. (2001)
pBB540	pSC101 *ori*, encoding *grpE*, *clpB* (cm^{r})	Tomoyasu et al. (2001)
pBB541	p15A *ori*, encoding *groELS* (spec^{r})	Tomoyasu et al. (2001)
pBB542	p15A *ori*, encoding *dnaKJ*, *groELS* (large amount) (spec^{r})	gift of B. Bukau
pBB550	p15A *ori*, encoding *dnaKJ* (large amount), *groELS* (spec^{r})	gift of B. Bukau

† cm^{r} …carrying canamycin resistant marker, spec^{r}… carrying spectomycin resistant marker

Table 2: Chaperone mutant strains used in this study.

Strain	Genotype	Phenotype	Reference
JGT3	MC4100 *ΔclpB::kan*	ClpB^{-}	Thomas and Baneyx, 1998
JGT6	MC4100 *zjd::T10 groES30*	GroES^{-}	Thomas and Baneyx, 1998
JGT20	MC4100 *dnaK756 thr::Tn10*	DnaK^{-}	Thomas and Baneyx, 1998
JGT32	MC4100 *dnaK756 thr::Tn10 ΔclpB::kan*	DnaK^{-} ClpB^{-}	Thomas and Baneyx, 1998
BB4564	MC4100 *groEL140 zjd::Tn10 zje::Ωspec^{r}/str^{r}*	GroEL^{-}	Mogk et al., 1999
BB4565	MC4100 *groEL44 zjd::Tn10 zje::kan*	GroEL^{-}	Mogk et al., 1999

Captions to Figures

Figure 1. Compositional analysis of the insoluble proteome of TG1:pλFGFB producing hFGF-2 (A, C) or TG1:pCYTEXP1 as control (B, D) six hours after temperature upshift from 30 to 42°C. Cells were grown in high-cell density cultures as described previously (Seeger et al., 1996). The insoluble proteins were separated by isoelectric focussing (A, B) or non-equilibrium pH-electrophoresis (C, D). Gels were stained with Coomassie-brilliant blue. Images are oriented with basic proteins to the left side. Identified spots include the heat-shock chaperone DnaK; the metabolic proteins D-tagatose-1,6-bisphosphate aldolase (GatY), Tryptophanase (TnaA), dihydrolipamide dehydrogenase (LpdA) and succinate dehydrogenase subunit A (SdhA); plasmid-encoded thermolabile repressor cI^{857}; the membrane proteins OmpA, OmpC and OmpF. Proteins only found in the insoluble cell fraction of hFGF-2-producing cells are encircled. Multiple spots in the lower left corner of (C) have been identified by N-terminal sequencing as variants of the recombinant protein hFGF-2. The expected positions of plasmid-encoded pre-β-lactamase (pre-β-Lac) and the small heat-shock protein IbpB are indicated in grey color. The basic protein hFGF-2 (pI 9.6) is not detected on equilibrium gels (A, B); the membrane proteins OmpA, OmpC and OmpF are not solubilized during sample preparation for non-equilibrium pH-electrophoresis (solubilisation of proteins in 9.5 M urea at room temperature) (C, D). The upper and lower dotted lines are drawn at the positions of approx. 30 and 75 kDa, respectively.

Figure 2. Thermodynamic and thermal stability of hFGF-2 in native and aggregated conformations. (A) Guanidinium-hydrochloride (Gdn-HCl) induced unfolding of native hFGF-2 at 25°C (solid circles, see also Estapé et al., 1998) and Gdn-HCl dependent disaggregation of aggregates obtained *in vitro* by thermal denaturation of purified hFGF-2 at 70°C (solid squares) or isolated as inclusion bodies (open squares). (B) Thermal denaturation of hFGF-2 in the presence (solid symbols) or absence (open symbols) of 100 mmol L^{-1} β-mercaptoethanol. Temperature was increased with a rate of 0.1 – 0.3°C min^{-1}.

Figure 3: Coproduction of hFGF-2 and the DnaKJ/GrpE system (*E. coli* MC4100 transformed with the three plasmids pλFGFB, pBB535, and pBB530). Cells were grown at 30°C in shake flasks on glucose-mineral salt medium. The synthesis of hFGF-2 was induced by temperature upshift to 42°C and the synthesis of DnaKJ/GrpE was started by the addition of IPTG to a final concentration of 0.5 mmol L^{-1}. (A) Only synthesis of hFGF2, (B) only synthesis of DnaKJ and GrpE (C), induction of DnaKJ and GrpE one hour after induction of hFGF-2 synthesis, and (D) induction of DnaKJ and GrpE one hour before induction of hFGF-2 synthesis by temperature upshift. Coomassie-stained SDS-PAGE of total (top), soluble (mid) and insoluble (bottom) cell fractions are shown. Time relative to the time of temperature upshift (A, C) or relative to IPTG addition (B, D), is given below the lanes. Positions of hFGF-2, DnaK, DnaJ, and GrpE as well as OmpA OmpC and OmpF are indicated by arrows on the right and molecular markers (in kDa) on the left. Please note that insoluble fractions are concentrated four times relative to soluble cell fractions.

Figure 4: Coproduction of hFGF2 and the GroELS system (*E. coli* MC4100 transformed with the three plasmids pλFGFB, pBB528, and pBB541). Cells were grown at 30°C in shake flasks on glucose-mineral salt medium. The synthesis of hFGF-2 was induced by temperature upshift to 42°C and the synthesis of GroELS was started by the addition of IPTG to a final concentration of 0.5 mmol L^{-1}. (A) Only synthesis of hFGF2, (B) only synthesis of GroELS (C), induction of GroELS one hour after induction of hFGF-2 synthesis, and (D) induction of GroELS one hour before induction of hFGF-2 synthesis by temperature upshift. Coomassie-stained SDS-PAGE of total (top), soluble (mid) and insoluble (bottom) cell fractions are shown. Time relative to the time of temperature upshift (A, C) or relative to IPTG addition (B, D), is given below the lanes. Positions of hFGF-2, GroEL and GroES as well as OmpA OmpC and OmpF are indicated by arrows on the right and molecular markers (in kDa) on the left. Please note that insoluble fractions are concentrated four times relative to soluble cell fractions.

Figure 5: Impact of combined chaperone coproduction on initial accumulation of hFGF-2 in soluble and inclusion body fractions. Cultures were incubated at 30°C, and synthesis of chaperones was induced by IPTG. Initial distribution of hFGF-2 one hour after induction by temperature upshift: total cell protein (black bars), inclusion body cell fraction (gray bars), and soluble cell fraction (white bars). Chaperones were induced one hour before hFGF-2 induction. The concentration of hFGF-2 was determined by densitometry of Coomassie-stained SDS-PAGE and is given relative to the concentration in a reference cultivation without chaperone coproduction at the same time. KJ corresponds to *E. coli* MC4100 transformed with the three plasmids pλFGFB, pBB530, and pBB535 coexpressing DnaKJ and GrpE; KJ-B to *E. coli* MC4100 transformed with the three plasmids pλFGFB, pBB540, and pBB535 coexpressing DnaKJ, GrpE and ClpB; KJ-B-ls to *E. coli* MC4100 transformed with the three plasmids pλFGFB, pBB540, and pBB550 coexpressing DnaKJ, GrpE, ClpB, and GroELS in small amounts; KJ-B-LS to *E. coli* MC4100 transformed with the three plasmids pλFGFB, pBB540, and pBB542 coexpressing DnaKJ, GrpE, ClpB, and GroELS in large amounts; and LS to *E. coli* MC4100 transformed with the three plasmids pλFGFB, pBB528, and pBB541 coexpressing GroELS in large amounts.

Figure 6. Impact of combined chaperone coproduction on longterm accumulationof hFGF-2 in soluble and inclusion body fraction. (A) Equilibrium concentration of hFGF-2 in soluble and (B) insoluble cell fractions (mean values of the relative concentrations 4-8 h after induction of hFGF-2 synthesis). Chaperones were induced one hour before (black bars) or one hours after (grey bars) the temperature shift for induction hFGF-2 production. The concentration of hFGF-2 were determined by densitometry of Coomassie-stained SDS-PAGE and are given relative to the concentration in a reference cultivation without chaperone coproduction at the same time. KJ corresponds to *E. coli* MC4100 transformed with the three plasmids pλFGFB, pBB530, and pBB535 coexpressing DnaKJ and GrpE; KJ-B to *E. coli* MC4100 transformed with the three plasmids pλFGFB, pBB540, and pBB535 coexpressing DnaKJ, GrpE and ClpB; KJ-B-ls to *E. coli* MC4100 transformed with the three plasmids pλFGFB, pBB540, and pBB550 coexpressing DnaKJ, GrpE, ClpB, and GroELS in small amounts; KJ-B-LS to *E. coli* MC4100 transformed with the three plasmids pλFGFB, pBB540, and pBB542 coexpressing DnaKJ, GrpE, ClpB, and GroELS in large amounts; and LS to *E. coli* MC4100 transformed with the three plasmids pλFGFB, pBB528, and pBB541 coexpressing GroELS in large amounts.

Fig. 7: Accumulation and folding of hFGF-2 in mutant strains. The amount of hFGF-2 three hours after induction by the temperature shift in the total cell protein (black bars), in the soluble (white bars) and insoluble (grey bars) cell fractions was analysed by SDS-PAGE and densitometry. hFGF-2 amount is expressed such that the area of total hFGF-2 in the wild type was taken as one and other values were related. (A) production in chaperonin mutants, (B) production in the other chaperone mutants.

References

Allen, S.P., Polazzi, J.O., Gierse, J.K., Easton, A.M., 1992. Two novel heat shock genes encoding proteins produced in response to heterologous protein expression in *Escherichia coli*. J. Bacteriol. 174, 6938-6947.

Baneyx, F., Palumbo, J.L., 2002. Improving heterologous protein folding via molecular chaperone and foldase co-expression. In: Vaillancourt, P.E. (Ed.), *E. coli* Gene Expression Protocols. Totowa, New Jersey: Humana Press, pp. 171-197.

Baneyx, F., Mujacic, M., 2004. Recombinant protein folding and misfolding in *Escherichia coli*. Nature Biotechnol. 22, 1399-1408.

Ben-Zvi, A.P., Goloubinoff, P., 2001. Review: Mechanism of disaggregation and refolding of stable protein aggregates by molecular chaperones. J. Struct. Biol. 135, 84-93.

Blum, P., Velligan, M., Lin, N., Matin, A., 1992. DnaK-mediated alterations in human growth hormone protein inclusion bodies. Bio/Technol. 10, 301-304.

Bukau, B., Horwich, A.L., 1998. The Hsp70 and Hsp60 chaperone machines. Cell 92, 351-366.

Carrió, M.M., Villaverde, A., 2001. Protein aggregation as bacterial inclusion bodies is reversible. FEBS Lett. 489, 29-33.

Carrió, M.M., Villaverde, A., 2003. Role of molecular chaperones in inclusion body formation. FEBS Lett. 537, 215-221.

Carrió, M.M., Villaverde, A., 2005. Localization of chaperones DnaK and GroEL in bacterial inclusion bodies. J. Bacteriol. 187, 3599-3601.

Carrió, M.M., Corchero, J.L., Villaverde, A., 1998. Dynamics of in vivo protein aggregation, building inclusion bodies in recombinant bacteria. FEMS Microbiol. Lett. 169, 9-15.

Carrió, M.M., Corchero, J.L., Villaverde, A., 1999. Proteolytic digestion of bacterial inclusion body proteins during dynamic transition between soluble and insoluble forms. Biochim. Biophys. Acta 1434, 170-176.

Carrió, M.M., Cubarsi, R., Villaverde A., 2000. Fine architecture of bacterial inclusion bodies. FEBS Lett. 471, 7-11.

Carrió, M.M., González-Montalbán, N., Vera, A., Villaverde, A., Ventura, S., 2005. Amyloid-like properties of bacterial inclusion bodies. J. Mol. Biol. 347, 1025-1037.

Cheng, Y.-S.E. (1983) Increased cell buoyant densities of protein overproducing *Escherichia coli* cells. Biochem. Biophys. Res. Commun. 111, 104-111.

Corchero, J.L., Cubarsí, R., Enfors, S.-O., Villaverde, A., 1997. Limited *in vivo* proteolysis of aggregated proteins. Biochem. Biophys. Res. Commun. 237, 325-330.

Cubarsí, R., Carrió, M.M., Villaverde, A., 2001. *In situ* proteolytic digestion of inclusion body ploypeptides occurs as a cascade process. Biochem. Biophys. Res. Commun. 282, 436-441.

de Marco, A., De Marco, V., 2004. Bacteria co-transformed with recombinant proteins and chaperones cloned in independent plasmids are suitable for expression tuning. J. Biotechnol. 109, 45-52.

Diamant, S., Ben-Zvi, A.P., Bukau, B., Goloubinoff, P., 2000. Size-dependent disaggregation of stable proteins aggregates by the DnaK chaperone machinery. J. Biol. Chem. 275, 21107-21113.

Estapé, D., Rinas, U., 1996. Optimized procedures for purification and solubilization of basic fibroblast growth factor inclusion bodies. Biotechnol. Tech. 10, 481-484.

Estapé, D., Rinas, U., 1999. Folding kinetics of the all-beta-sheet protein human basic fibroblast growth factor, a structural homolog of interleukin-1β. J. Biol. Chem. 274, 34083-34088.

Estapé, D., van den Heuvel, J., Rinas, U., 1998. Susceptibility towards intramolecular disulphide-bond formation affects conformational stability and folding of human basic fibroblast growth factor. Biochem. J. 335, 343-349.

Georgiou, G., Valax, P., 1996. Expression of correctly folded proteins in *Escherichia coli*. Curr. Opin. Biotechnol. 7, 190-197.

Gonzáles-Montalbán, N., Carrió, M.M., Cuatrecasas, S., Arís, A., Villaverde, A., 2005. Bacterial inclusion bodies are cytotoxic in vivo in absence of functional chaperons DnaK or GroEL. J. Biotechnol. 118, 406-412.

Goloubinoff, P., Gatenby, A.A., Lorimer, G.H., 1989. GroE heat-shock proteins promote assembly of foreign prokaryotic ribulose bisphosphate carboxylase oligomers in *Escherichia coli*. Nature 337, 44-47.

Goloubinoff, P., Mogk, A., Ben-Zvi, A.P., Tomoyasu, T., Bukau, B., 1999. Sequential mechanism of solubilization and refolding of stable protein aggregates by a bichaperone network. Proc. Natl. Acad. Sci. USA 96, 13732-13737.

Hart, R.A., Rinas, U., Bailey, J.E., 1990. Protein composition of *Vitreoscilla* hemoglobin inclusion bodies produced in *Escherichia coli*. J. Biol. Chem. 265, 12728-12733.

Hoffmann, F., Rinas, U., 2000. Kinetics of heat-shock response and inclusion body formation during temperature-induced production of basic fibroblast growth factor in high-cell density cultures of recombinant *Escherichia coli*. Biotechnol. Prog. 16, 1000-1007.

Hoffmann, F., Rinas, U., 2001a. Plasmid amplification in *Escherichia coli* after temperature upshift is impaired by induction of recombinant protein synthesis. Biotechnol. Lett. 23, 1819-1825.

Hoffmann, F., Rinas, U., 2001b. On-line estimation of the metabolic burden resulting from synthesis of plasmid-encoded and heat-shock proteins in high-cell density cultures of recombinant *Escherichia coli*. Biotechnol. Bioeng. 76, 333-340.

Hoffmann, F., Posten, C., Rinas, U., 2001. Kinetic model of in vivo folding and inclusion body formation in recombinant *Escherichia coli*. Biotechnol Bioeng. 72, 315-322.

Hoffmann, F., Weber, J., Rinas, U., 2002. Metabolic adaptation of *Escherichia coli* during temperature-induced recombinant protein synthesis, 1. Synthesis kinetics of catabolic enzymes. Biotechnol. Bioeng. 80, 313-319.

Houry, W.A., Frishman, D., Eckerskorn, C., Lottspeich, F., Hartl, F.U., 1999. Identification of *in vivo* substrates of the chaperonin GroEL. Nature 402, 147-154.

Kandror, O., Busconi, L., Sherman, M., Goldberg, A.L., 1994. Rapid degradation of an abnormal protein in *Escherichia coli* involves the chaperones GroEL and GroES. J. Biol. Chem. 269, 23575-23582.

Kandror, O., Sherman, M., Goldberg, A., 1999. Rapid degradation of an abnormal protein in *Escherichia coli* proceeds through repeated cycles of association with GroEL. J. Biol. Chem. 274, 37743-37749.

Kane, J.F., Hartley, D.L., 1991. Properties of recombinant protein-containing inclusion bodies in *Escherichia coli*. In: Seetharam, R. und Sharma, S.K. (Eds.), Purification and analysis of recombinant proteins. Marcel Dekker Inc, New York Basel Hong Kong, pp. 121-145.

Kędzierska, S., Matuszewska, E., 2001. The effect of co-overproduction of DnaK/DnaJ/GrpE and ClpB proteins on the removal of heat-aggregated proteins from *Escherichia coli* Δ*clpB* mutant cells - new insight into the role of Hsp70 in a functional cooperation with Hsp100. FEMS Microbiol. Lett. 204, 355-360.

Kędzierska, S., Staniszewska, M., Węgrzyn, A., Taylor, A., 1999. The role of DnaK/DnaJ and GroEL/GroEL systems in the removal of endogenous proteins aggregated by heat-shock from *Escherichia coli* cells. FEBS Lett. 446, 331-337.

Kędzierska, S., Jezierski, G., Taylor, A., 2001. DnaK/DnaJ chaperone system system reactivates endogenous *E. coli* thermostable FBP aldolase in vivo and in vitro, the effect is enhanced by GroE heat shock proteins. Cell Stress Chaperones 6, 29-37.

Korz, D.J., Rinas, U., Hellmuth, K., Sanders, E.A., Deckwer, W.-D., 1995. Simple fed-batch technique for high-cell density cultivation of *Escherichia coli*. J. Biotechnol. 39, 59-65.

Laskowska, E., Kuczynska-Wisnik, D., Skorko-Glonek, J., Taylor, A., 1996. Degradation by protease Lon, Clp and HtrA, of *Escherichia coli* proteins aggregated *in vivo* by heat shock, HtrA protease action *in vivo* and *in vitro*. Mol. Microbiol. 22, 555-571.

Lee, S.C., Olins, P.O., 1992. Effect of overproduction of heat shock chaperones GroESL and DnaK on human procollagenase production in *Escherichia coli*. J. Biol. Chem. 267, 2849-2852.

LeThanh, H., Hoffmann, F., 2005. Processes for production of active α-glucosidase by in-vivo-reactivation from inclusion bodies. Evaluation of processes using in vivo reactivation from inclusion bodies. Biotechnol. Prog. 21, 1053-1061.

Malki, A., Caldas, T., Parmeggiani, A., Kohiyama, M., Richarme, G., 2002. Specificity of elongation factor EF-TU for hydrophobic peptides. Biochem. Biophys. Res. Commun. 296, 749-754.

Mogk, A., Tomoyasu, T., Goloubinoff, P., Rüdiger, S., Röder, D., Langen, H., Bukau, B., 1999. Identification of thermolabile *Escherichia coli* proteins: Prevention and reversion of aggregation by DnaK and ClpB. EMBO J. 18, 6934-6949.

Mogk, A., Deuerling, E., Vorderwülbecke, S., Vierling, E., Bukau, B., 2003a. Small heat shock proteins, ClpB and the DnaK system form a functional triade in reversing protein aggregation. Mol. Microbiol. 50, 585-595.

Mogk, A., Schlieker, C., Friedrich, K.L., Schönfeld, H.J., Vierling, E., Bukau, B., 2003b. Refolding of substrates bound to small Hsps relies on a disaggregation reaction mediated most efficiently by ClpB/DnaK. J. Biol. Chem. 278, 31033-31042.

Mujacic, M., Bader, M.W., Baneyx, F., 2004. *Escherichia coli* Hsp31 functions as a holding chaperone that cooperates with the DnaK-DnaJ-GrpE system in the management of protein misfolding under severe stress conditions. Mol. Microbiol. 51, 849-859.

Nishihara, K., Kanemori, M., Kitagawa, M., Yanagi, H., Yura, T., 1998. Chaperone coexpression plasmids: differential and synergistic roles of DnaK-DnaJ-GrpE and GroEL-GroES in assisting folding of an allergen of japanse cedar pollen, Cryj2, in *Escherichia coli*. Appl. Environ. Microbiol. 64, 1694-1699.

Oberg, K., Chrunyk, B.A., Wetzel, R., Fink, A.L., 1994. Nativelike secondary structure in interleukin-1β inclusion bodies by attenuated total reflectance FTIR. Biochemistry 33, 2628-2634.

Patzelt, H., Rüdiger, S., Brehmer, D., Kramer, G., Vorderwülbecke, S., Schaffitzel, E., Waitz, A., Hesterkamp, T., Dong, L., Schneider-Mergener, J., Bukau, B., Deuerling, E., 2001. Binding specificity of *Escherichia coli* trigger factor. Proc. Natl. Acad. Sci. USA 98, 14244-14249.

Rinas, U., Bailey J.E., 1992. Protein compositional analysis of inclusion bodies produced in recombinant *Escherichia coli*. Appl. Microbiol. Biotechnol. 37, 609-614.

Rinas, U., Bailey J.E., 1993. Overexpression of bacterial hemoglobin causes incorporation of pre-β-lactamase into cytoplasmic inclusion bodies. Appl. Environ. Microbiol. 59, 561-566.

Rüdiger, S., Germeroth, L., Schneider-Mergener, J., Bukau, B., 1997. Substrate specifity of the DnaK chaperone determined by screening cellulose-bound peptide libraries. EMBO J. 16, 1501-1507.

Sakikawa, C., Taguchi, H., Makino, Y., Yoshida, M., 1999. On the maximum size of proteins to stay and fold in the cavity of GroEL underneath GroES. J. Biol. Chem. 274, 21251-21256.

Sato, K., Sato, M.H., Yamaguchi, A., Yoshida, M., 1994. Tetracycline/H+ antiporter was degraded rapidly in *Escherichia coli* cells when truncated at last transmembrane helix and this degradation was protected by overproduced GroEL/ES. Biochem. Biophys. Res. Commun. 202, 258-264.

Schrödel, A., de Marco, A., 2005. Characterization of the aggregates formed during recombinant protein expression in bacteria. BMC Biochemistry 6, 10.

Schröder, H., Langer, T., Hartl, F.U., Bukau, B., 1993. DnaK, DnaJ and GrpE form a cellular chaperone machinery capable of repairing heat-induced protein damage. EMBO J. 12, 4137-4144.

Seeger A., Rinas U., 1996. Two-step chromatographic procedure for purification of basic fibroblast growth factor from recombinant *Escherichia coli* and characterization of the equilibrium parameters of adsorption. J. Chromatogr. A 746, 17-24.

Seeger, A., Schneppe, B., McCarthy, J.E.G., Deckwer, W.-D., Rinas, U., 1995. Comparison of temperature- and isopropyl-β-D-thiogalacto-pyranosid-induced synthesis of basic fibroblast growth factor in high-cell density cultures of recombinant *Escherichia coli*. Enzyme Microb. Technol. 17, 947-953.

Sherman, M.Y.S., Goldberg, A.L., 1996. Involvement of molecular chaperones in intracellular protein breakdown. In: Feige, U., Morimoto, R.I., Yahara, I., Polla, B. (Eds.), Stress-inducible cellular responses. Birkhäuser Verlag, Basel (Switzerland), pp. 57-78.

Taylor, G., Hoare, M., Gray, D.R., Marston, F.A.O., 1986. Size and density of protein inclusion bodies. Bio/Technology 4, 553-557.

Teter, S.A., Houry, W.A., Ang, D., Tradler, T., Rockabrand, D., Fischer, G., Blum, P., Georgopoulos, C., Hartl. F.U., 1999. Polypeptide flux through bacterial Hsp70: DnaK cooperates with trigger factor in chaperoning nascent chains. Cell 97, 755-765.

Thomas, J.G., Baneyx, F., 1998. Roles of the *Escherichia coli* small heat shock proteins IbpA and IbpB in thermal stress management: comparison with ClpA, ClpB, and HtpG in vivo. J. Bacteriol. 180, 5165-5172.

Thomas, J.G., Baneyx, F., 2000. ClpB and HtpG facilitate *de novo* protein folding in stressed *Escherichia coli* cells. Mol. Microbiol. 36, 1360-1370.

Tomoyasu, T., Mogk, A., Langen, H., Goloubinoff, P., Bukau, B., 2001. Genetic dissection of the roles of chaperones and proteases in protein folding and degradation in the *Escherichia coli* cytosol. Mol. Microbiol. 40, 397-413.

Valax, P., Georgiou, G., 1993. Molecular characterization of β-lactamase inclusion bodies produced in *Escherichia coli* 1. Composition. Biotechnol. Prog. 9, 539-547.

Ventura, S., Villaverde, A., 2006. Protein quality in bacterial inclusion bodies. Trends Biotechnol. 24, 179-185.

Vera, A., Aris, A., Carrio, M., Gonzalez-Montalban, N., Villaverde, A., 2005. Lon and ClpP proteases participate in the physiological disintegration of bacterial inclusion bodies. J. Biotechnol. 119, 163-71.

Vorderwülbecke, S., Kramer, G., Merz, F., Kurz, T.A., Rauch, T., Zachmann-Brand, B., Bukau, B., Deuerling, E., 2004. Low temperature or GroEL/ES overproduction permits growth of *Escherichia coli* cells lacking trigger factor and DnaK. FEBS Lett. 559, 181-187.

Watanabe, Y.H., Motohashi, K., Taguchi, H., Yoshida, M., 2000. Heat-inactivated proteins managed by DnaKJ-GrpE-ClpB chaperones are released as a chaperonin-recognizable non-native form. J. Biol. Chem. 275, 12388-12392.

Weibezahn, J., Bukau, B., Mogk, A., 2004. Unscrambling an egg: protein disaggregation by AAA+ proteins. Microb. Cell Fact. 3,1.

Weibezahn, J., Schlieker, C., Tessarz, P., Mogk, A., Bukau, B., 2005. Novel insights into the mechanism of chaperone-assisted protein disaggregation. Biol. Chem. 386, 739-744.

Zolkiewski, M., 1999. ClpB cooperates with DnaK, DnaJ, and GrpE in suppressing protein aggregation. J. Biol. Chem. 274, 28083-28086.

5

Fig. 1

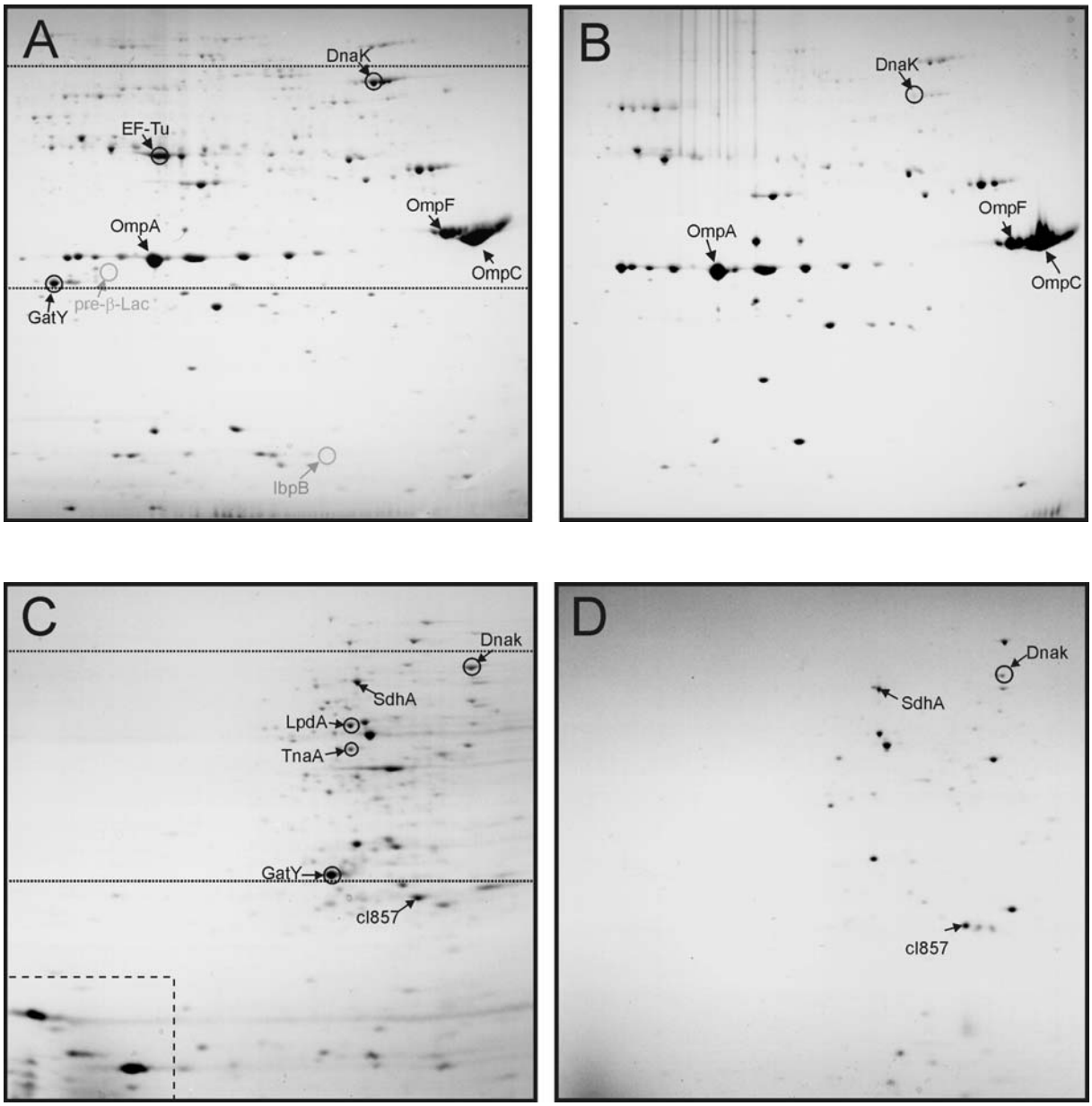
A
DnaK
EF-Tu
OmpF
OmpA
OmpC
GatY
pre-β-Lac
IbpB
B
DnaK
OmpF
OmpA
OmpC
C
Dnak
SdhA
LpdA
TnaA
GatY
cI857
D
Dnak
SdhA
cI857

Fig. 2

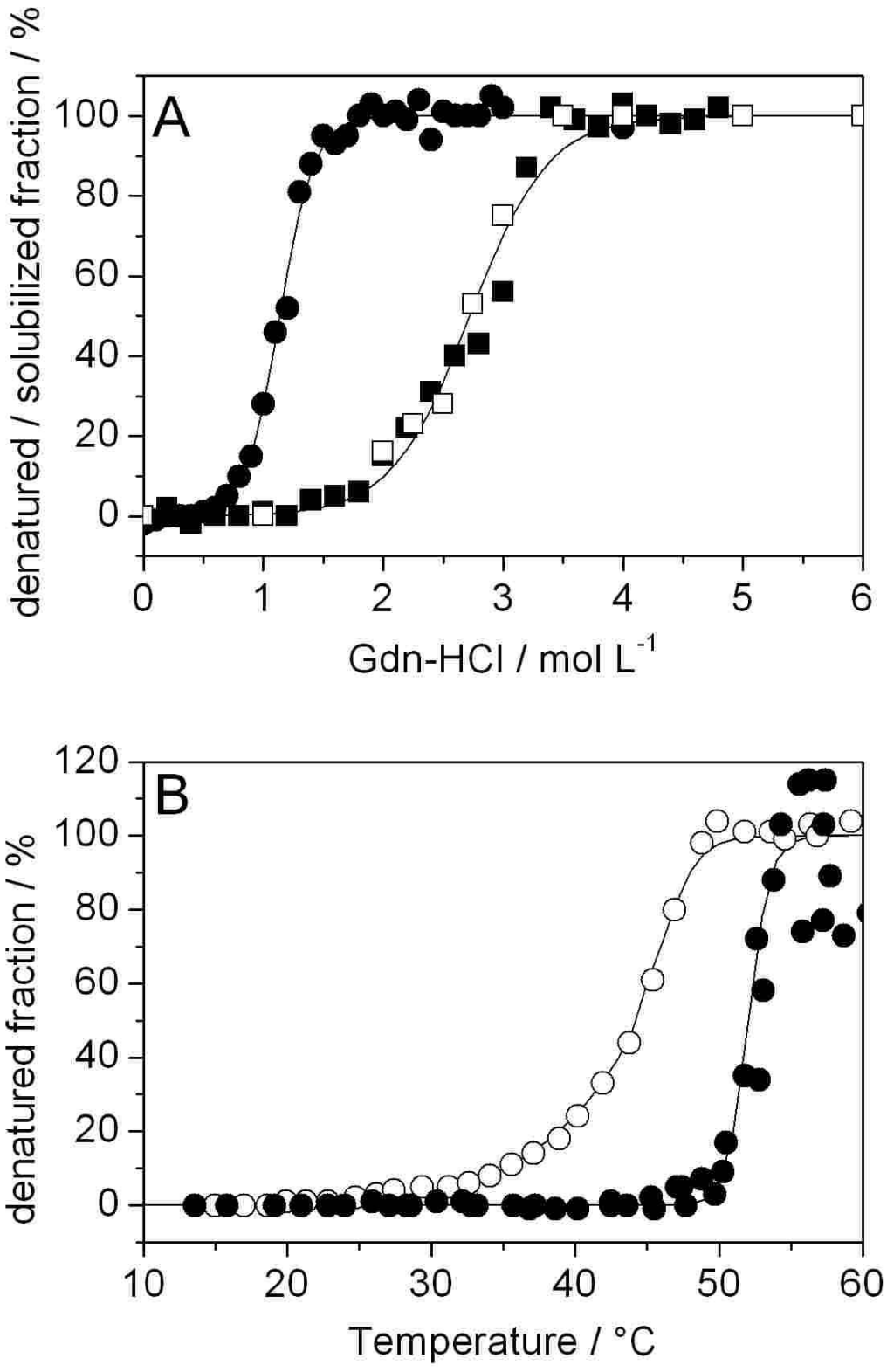
A
denatured / solubilized fraction / %
100
80
60
40
20
0
0
1
2
3
4
5
6
Gdn-HCl / mol L-1
B
denatured fraction / %
120
100
80
60
40
20
0
10
20
30
40
50
60
Temperature / °C

Fig. 3

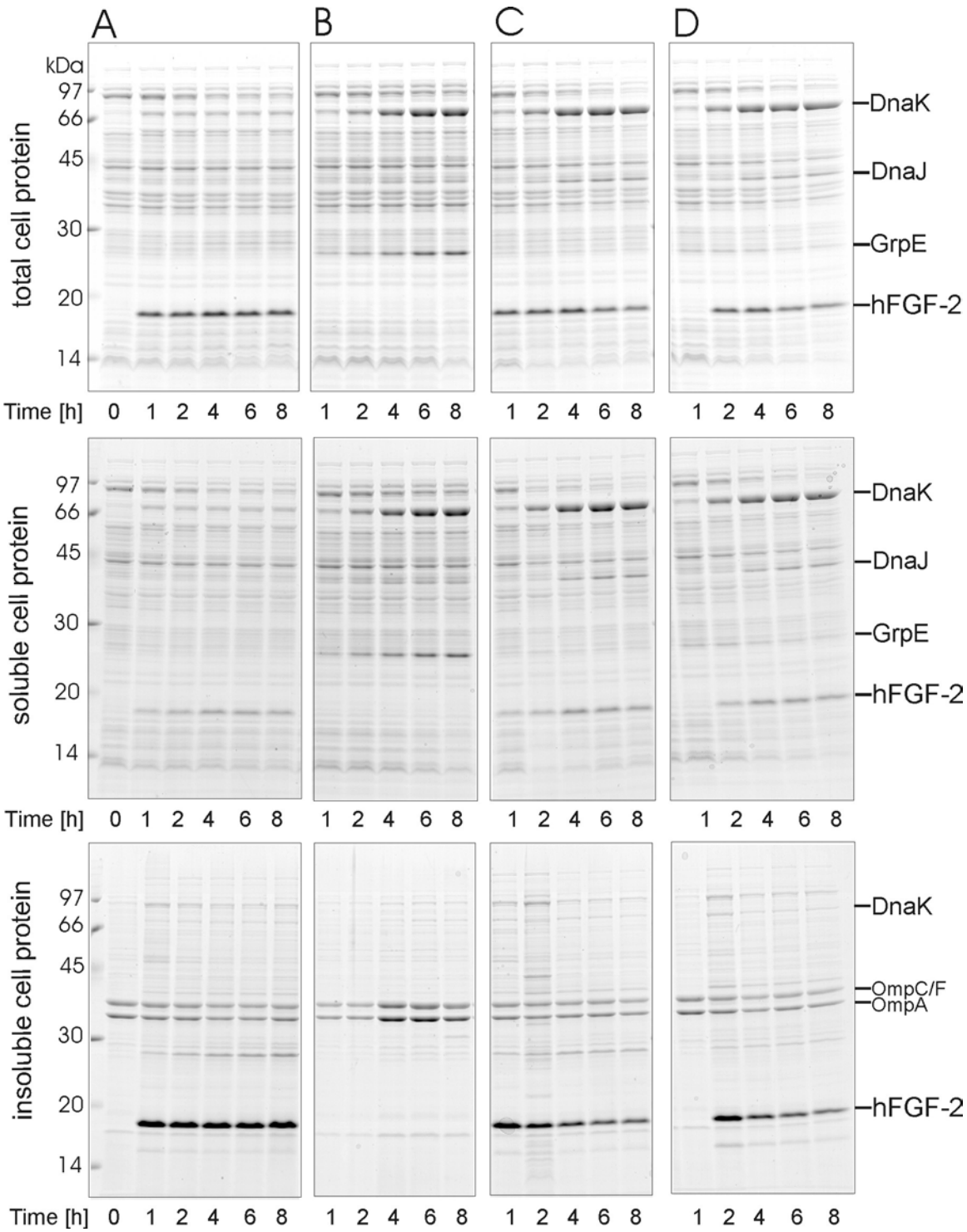
A
B
C
D
kDa
97
66
45
30
20
14
total cell protein
soluble cell protein
insoluble cell protein
Time [h]
0 1 2 4 6 8
1 2 4 6 8
DnaK
DnaJ
GrpE
hFGF-2
OmpC/F
OmpA

Fig. 4

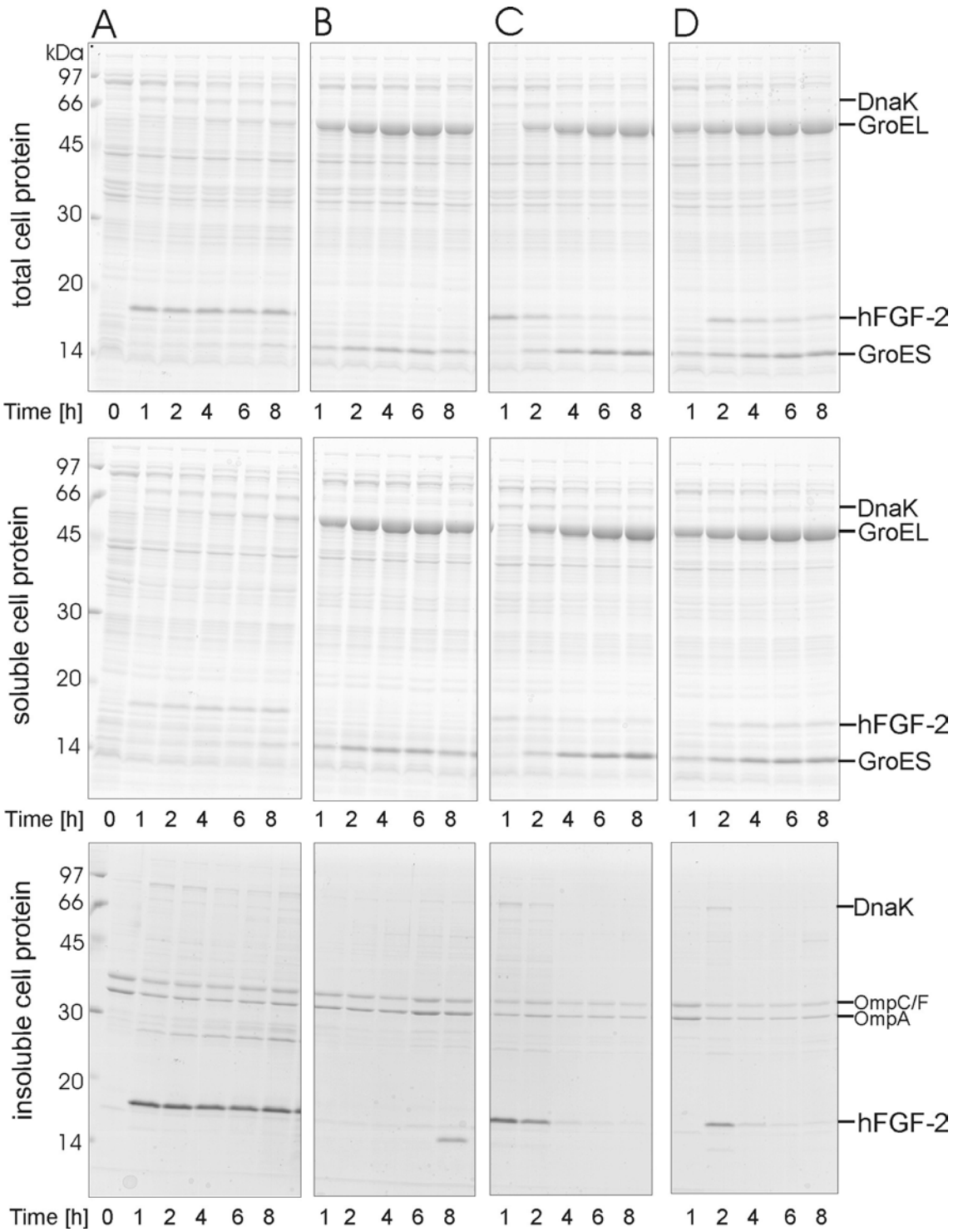
A
B
C
D
kDa
97
66
45
30
20
14
total cell protein
DnaK
GroEL
hFGF-2
GroES
Time [h] 0 1 2 4 6 8 1 2 4 6 8 1 2 4 6 8 1 2 4 6 8
soluble cell protein
insoluble cell protein
OmpC/F
OmpA

Fig. 5

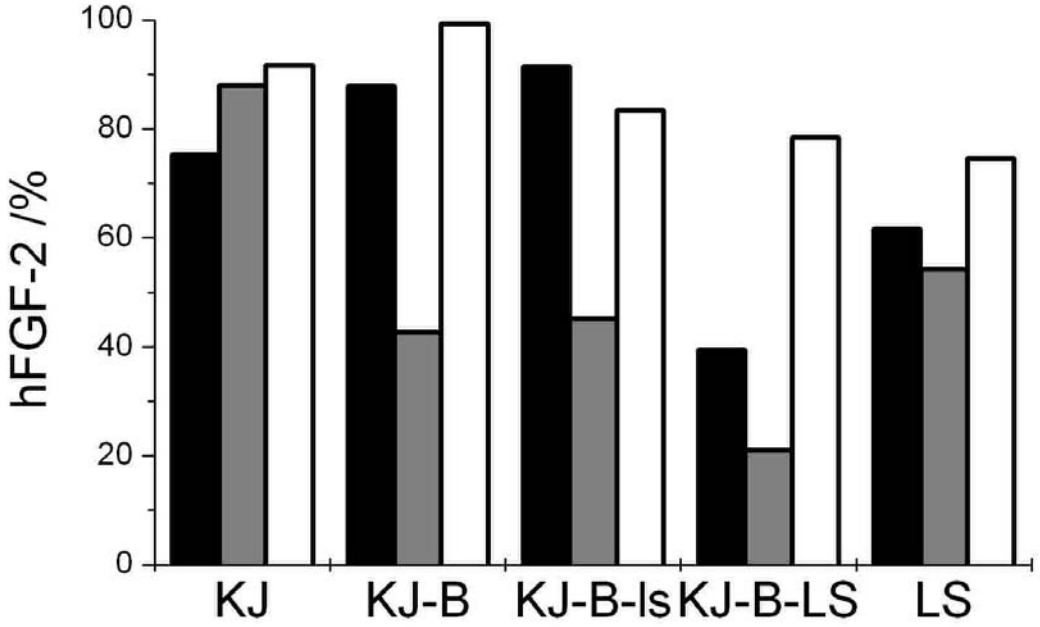

Fig. 6

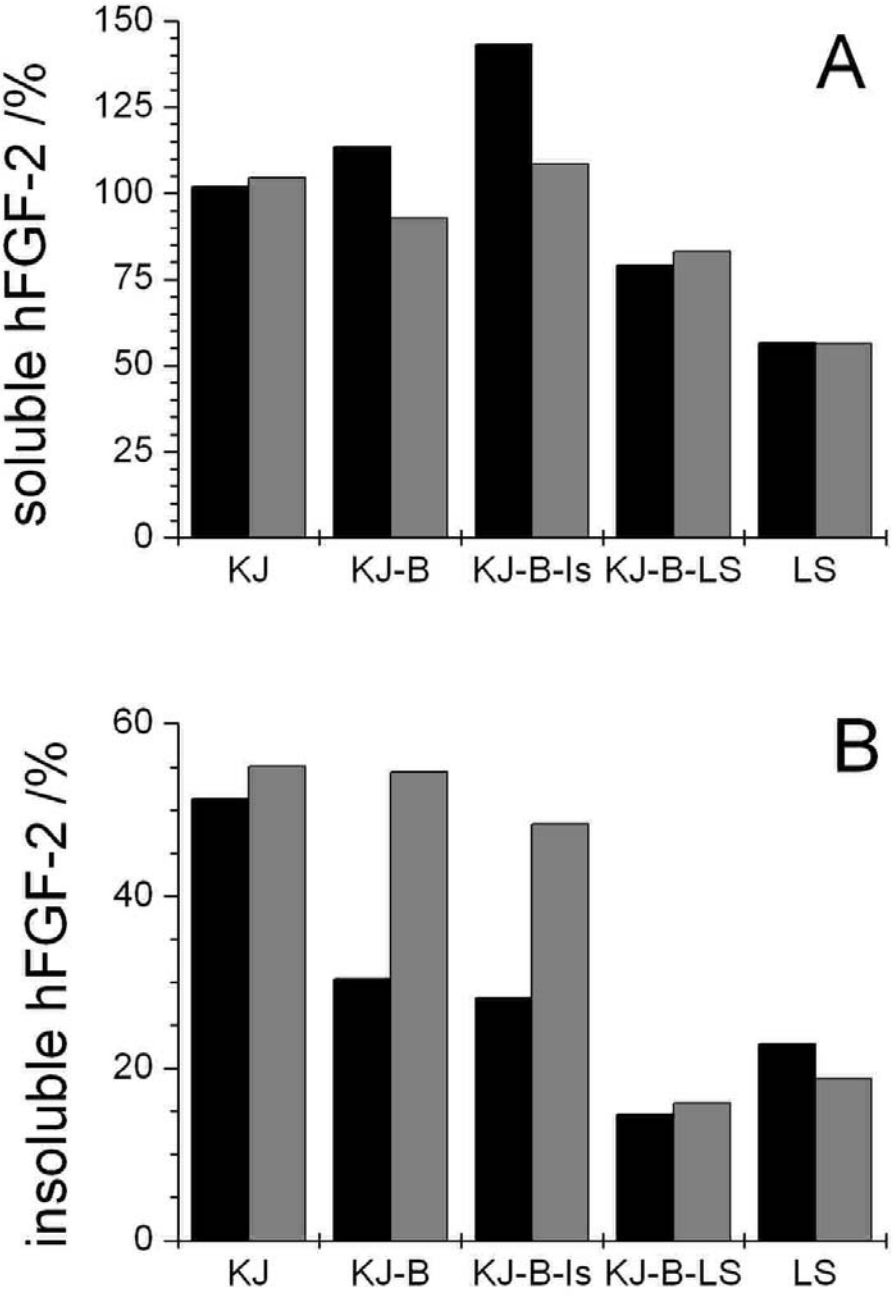
A
soluble hFGF-2 /%
150
125
100
75
50
25
0
KJ
KJ-B
KJ-B-Is
KJ-B-LS
LS
B
insoluble hFGF-2 /%
60
40
20
0
KJ
KJ-B
KJ-B-Is
KJ-B-LS
LS

Fig. 7

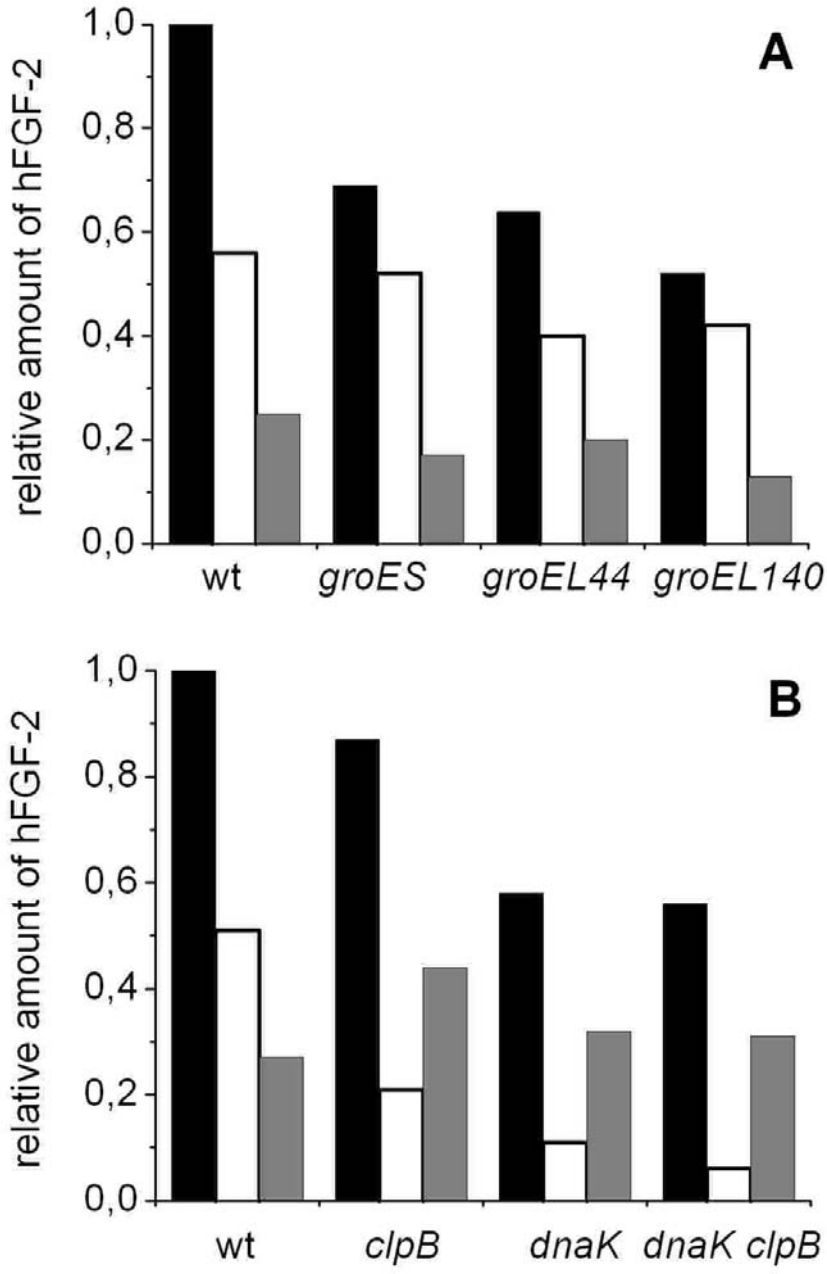
A
relative amount of hFGF-2
1,0
0,8
0,6
0,4
0,2
0,0
wt
groES
groEL44
groEL140
B
relative amount of hFGF-2
1,0
0,8
0,6
0,4
0,2
0,0
wt
clpB
dnaK
dnaK clpB